



A presequence- and voltage-sensitive channel of the mitochondrial preprotein translocase formed by Tim23

Kaye N. Truscott^{1,2}, Peter Kovermann¹⁻³, Andreas Geissler¹, Alessio Merlin^{1,4}, Michiel Meijer⁵, Arnold J.M. Driessen⁶, Joachim Rassow⁷, Nikolaus Pfanner¹ and Richard Wagner³

Published online: 19 November 2001, DOI: 10.1038/nsb726

Proteins imported into the mitochondrial matrix are synthesized in the cytosol with an N-terminal presequence and are translocated through hetero-oligomeric translocase complexes of the outer and inner mitochondrial membranes. The channel across the inner membrane is formed by the presequence translocase, which consists of roughly six distinct subunits; however, it is not known which subunits actually form the channel. Here we report that purified Tim23 forms a hydrophilic, ~13–24 Å wide channel characteristic of the mitochondrial presequence translocase. The Tim23 channel is cation selective and activated by a membrane potential and presequences. The channel is formed by the C-terminal domain of Tim23 alone, whereas the N-terminal domain is required for selectivity and a high-affinity presequence interaction. Thus, Tim23 forms a voltage-sensitive high-conductance channel with specificity for mitochondrial presequences.

Nuclear-encoded proteins destined for the mitochondrion must be translocated from the cytosol through an outer and inner membrane to reach the mitochondrial matrix. Two distinct protein complexes are essential for this process: the translocase of the outer membrane (TOM complex) and a translocase of the inner membrane specific for preproteins containing a mitochondrial presequence (TIM23 complex)¹⁻⁴. The essential protein Tom40 forms a continuous hydrophilic channel in the outer membrane that allows preproteins to pass across the membrane^{5,6}. Other known Tom components function as receptors for preprotein recognition or in the assembly and stability of the TOM complex. Preproteins are translocated through the inner membrane by the TIM23 complex, which consists of the essential integral membrane proteins Tim23 and Tim17, the membrane-bound Tim44 with the associated matrix heat shock protein mtHsp70, and probably additional translocation components^{1-4,7-12}. Translocation of the presequence requires a membrane potential ($\Delta\psi$) across the inner membrane, whereas an ATP-dependent motor system that includes mtHsp70 and its membrane anchor Tim44 drives the translocation of the mature portions of preproteins into the matrix¹⁻⁴. Patch-clamp analysis has suggested that the mitochondrial inner membrane has a presequence-sensitive channel^{8,11}. The identity of the channel-forming Tim protein(s) is not known, however, and thus the properties of the channel have not been characterized at the molecular level. Here we report the reconstitution and functional characterization of purified Tim23 and provide direct evidence that Tim23 forms the presequence-sensitive translocation channel of the mitochondrial inner membrane.

Tim23 forms a presequence-sensitive channel

We expressed *Saccharomyces cerevisiae* Tim23 (refs 13,14) at high levels in *Escherichia coli* cells, where it accumulated as inclusion bodies (Fig. 1a, lanes 3 and 4). We denatured these with urea and purified Tim23 to homogeneity (Fig. 1a, lane 5), then renatured the protein by diluting the urea in the presence of the nonionic detergent nonanoyl-N-methylglucamide (Mega-9) and azolectin and reconstituted it into liposomes⁵. We fused the liposomes with a planar bilayer and detected single-channel currents (Fig. 1b). In contrast, reconstitution of control proteins such as two other polytopic inner membrane proteins, Tim18 and Tim54 (refs 2,3), did not produce channel activity (unpublished data). The main single-channel conductance state of Tim23 in symmetrical 250 mM KCl revealed $\Lambda = 450 \pm 11$ pS in a linear current–voltage relationship (Fig. 1c). Smaller subconductance states were also present (Fig. 1b), most prominently $\Lambda = 140 \pm 15$ pS. The main conductance states were observed in multiples of three. The gating of these main conductance states occurred largely independently of each other; however, coupled transitions were also observed, including simultaneous closing of two main conductance states (Fig. 1b, lower part). Thus, the Tim23 channel exhibits a complex gating behavior covering a wide range of conductance states, from 140 pS to 450 pS and 1.35 nS and combinations of these values. In asymmetric buffer, the reversal potential of the main conductance state was $E_{rev} = 49.6 \pm 3.06$ mV (Fig. 1d), indicating that the Tim23 channel is highly selective for cations ($P_{K^+}:P_{Cl^-} = 16:1$). Upon a rapid increase of the membrane voltage, the number of open channels increased (Fig. 1b). Quantification revealed that after the onset of the voltage increase, the number of open channels rose expo-

¹Institut für Biochemie und Molekularbiologie, Universität Freiburg, Hermann-Herder-Strasse 7, D-79104 Freiburg, Germany. ²These authors contributed equally to this work. ³Biophysik, Universität Osnabrück, FB Biologie/Chemie, D-49034 Osnabrück, Germany. ⁴Present address: Schering AG, D-13342 Berlin, Germany. ⁵Section for Plant Pathology, Swammerdam Institute for Life Sciences, University of Amsterdam, 1098 SM Amsterdam, The Netherlands. ⁶Department of Microbiology, Groningen Biomolecular Sciences and Biotechnology Institute, University of Groningen, 9751 NN Haren, The Netherlands. ⁷Universität Hohenheim, Institut für Mikrobiologie, D-70593 Stuttgart, Germany.

Correspondence should be addressed to N.P. email: pfanner@uni-freiburg.de or R.W. email: wagner@uos.de

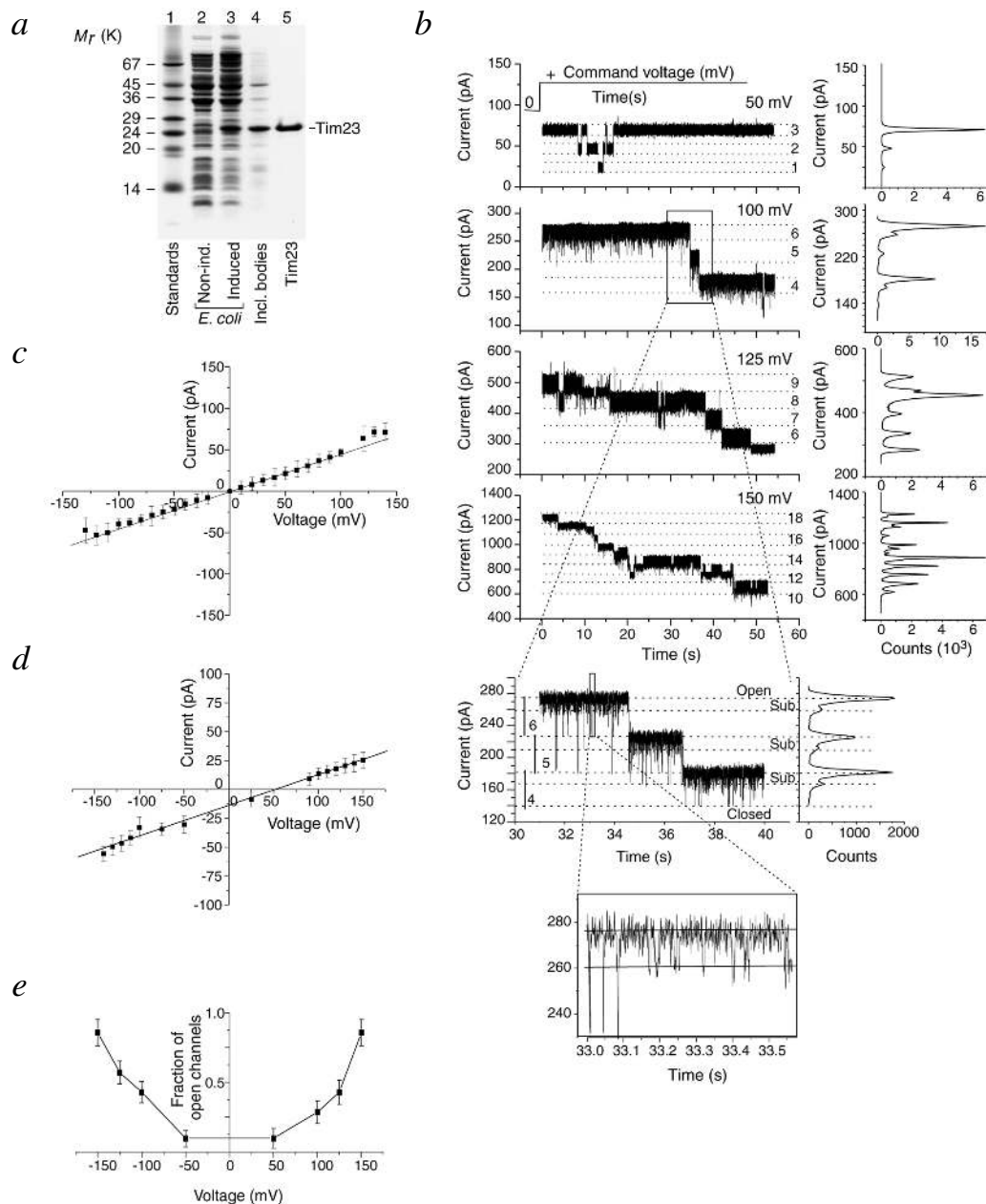


Fig. 1 Reconstituted Tim23 forms a cation-selective, voltage-sensitive channel. **a**, Expression and purification of recombinant Tim23 analyzed by SDS-PAGE with Coomassie brilliant blue staining. Lane 1, molecular size markers; lane 2, lysate from noninduced *E. coli* cells; lane 3, lysate from induced *E. coli* cells; lane 4, purified inclusion bodies; lane 5, purified Tim23. **b**, Current recordings at different membrane potentials from a bilayer containing 18 active channels, with corresponding amplitude histograms shown on the right. Applied membrane potentials are indicated. The buffer on both sides of the bilayer was 250 mM KCl, 0.1 mM CaCl_2 , 10 mM MOPS-Tris, pH 7.0. Two timescale-magnified traces originating from the indicated panels are shown underneath. **c**, Current-voltage relationship of a single channel deduced from single-channel currents of the main conductance state (buffer as in **b**). Data points are averages of five independent bilayers, with error bars representing the standard deviation. **d**, Current-voltage relationship of a single channel deduced from single-channel currents of the main conductance state in asymmetric buffers consisting of 0.1 mM CaCl_2 , 10 mM MOPS-Tris, pH 7.0 with 250 mM KCl (*cis*) / 20 mM KCl (*trans*). **e**, Fraction of Tim23 channels in an open state in relation to applied voltage. After application of different voltage steps at $t = 0$, mean currents were calculated for a time period of 10 s (from $t = 2$ s to $t = 12$ s). Data were normalized with respect to the maximal mean current at $V_m = 200$ mV. Data points are averages from three independent bilayers.

nentially with membrane potential (Fig. 1e). However, the Tim23 channels showed a tendency to close during prolonged application of a constant voltage (Fig. 1b, later time points) or in response to a slowly increasing voltage ramp (see below; Fig. 2a). Thus, the Tim23 channel can be activated by a rapid increase in membrane voltage but closes slowly during prolonged exposure to a membrane potential.

To determine if the activity of the Tim23 channel is influenced by mitochondrial presequences, we used a synthetic peptide corresponding to the presequence of cytochrome *c* oxidase subunit IV (CoxIV)¹⁵. CoxIV affected the channel conductance in a concentration-dependent manner. Even at only 20 nM, CoxIV elicited a strong response (Fig. 2a), but only from one side of the planar lipid bilayer. When CoxIV was added to the opposite side

articles

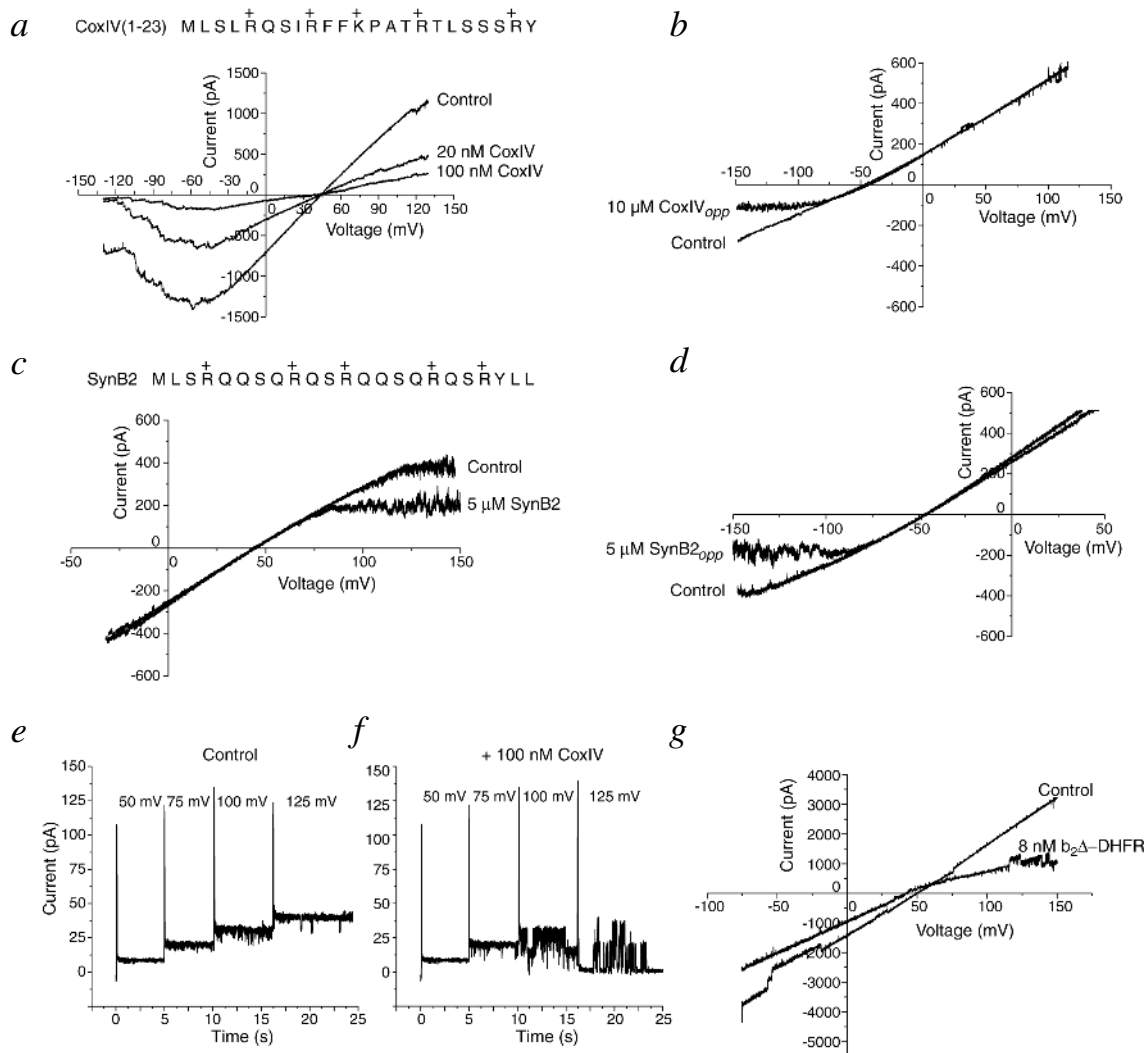


Fig. 2 The Tim23 channel is specifically influenced by a mitochondrial presequence. **a–d**, Comparison of the current–voltage relationship from bilayers containing several copies of active Tim23 channels in the absence (control) or presence of peptides (CoxIV and SynB2). The buffer was 10 mM MOPS-Tris, pH 7.0, 0.1 mM CaCl₂ with a salt gradient across the membrane of 250 mM KCl (*cis*)/20 mM KCl (*trans*) (**a,c**) or the reverse (**b,d**). The sweep rate of the command voltage was 1 mV s⁻¹. **a**, Addition of presequence peptide CoxIV to the *trans* side of the membrane. **b**, Addition of CoxIV peptide to the *cis* side of the membrane. At peptide concentrations below 1 μM, the current–voltage relationships were superimposable with the control trace. **c**, Addition of the peptide SynB2 to the *trans* side of the membrane. At concentrations below 1 μM, the current–voltage relationships were superimposable with the control trace without peptide. **d**, Addition of SynB2 to the *cis* side of the membrane. Single-channel current recordings in response to a voltage step protocol in the **e**, absence and **f**, presence of 100 nM CoxIV (*trans/cis*). Applied membrane potentials are indicated. Symmetrical ionic buffer conditions were used as described (Fig. 1b). **g**, Current–voltage relationship of a bilayer containing 25–30 active copies of the Tim23 channel in the absence (control) and presence of 8 nM b₂Δ-DHFR (*cis* and *trans*). Asymmetric ionic conditions and measurements used were as described for (a).

of the bilayer, micromolar concentrations were needed to influence the channel (Fig. 2b). This indicates that Tim23 was inserted into the small unilamellar liposomes in an asymmetrical orientation, as has previously been observed for other reconstituted channels, including Tom40 (refs 5,16). As a control, we used the peptide SynB2, which has an amino acid composition similar to that of CoxIV, including an equal number of positively charged residues (Fig. 2c), but does not function as a specific mitochondrial targeting signal¹⁵. SynB2 influenced the Tim23 channel activity only in micromolar concentrations, independent of the side to which it was added (Fig. 2c,d). The effect of CoxIV on the channel activity was voltage dependent, because the peptide induced a rapid gating (flickering) of the channel only above a threshold potential of ~100 mV (Fig. 2f). We conclude that the presequence peptide specifically influences the

channel activity through a high-affinity interaction with one side of Tim23 and that a rapid gating of the channel is activated by a combined action of both presequence and membrane potential.

To investigate whether the reconstituted Tim23 could interact with an entire mitochondrial preprotein, we used a purified presequence-containing model protein, b₂Δ-DHFR⁵. This preprotein affected the Tim23 channel more strongly than did the presequence peptide: just 8 nM preprotein induced both a rapid voltage-dependent inhibition of the channel and a shift of the reversal potential to $E_{rev} = 41 \pm 2.7$ mV ($P_{K^+}:P_{Cl^-} = 8.5:1$) (Fig. 2g). Thus, like Tom40 (ref. 5), recombinant Tim23 may achieve at least partial translocation of the preprotein.

It has been reported that *tim23-1* mitochondria, which contain a mutant form of Tim23 with a single amino acid substitu-

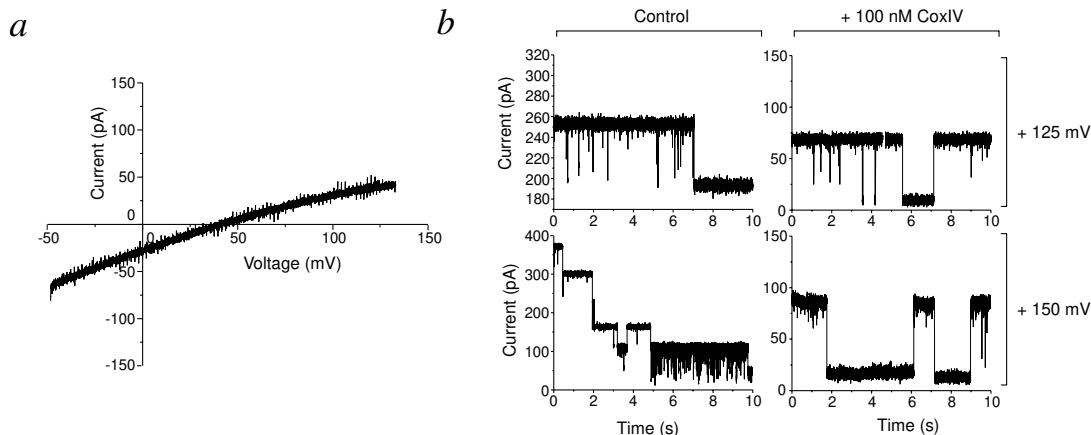


Fig. 3 Reduction of the presequence sensitivity in the mutant protein Tim23-1. **a**, Current–voltage relationship of the channel formed by the reconstituted mutant protein, Tim23-1, under asymmetric ionic conditions as outlined in Fig 2a. **b**, Current recordings from a bilayer containing reconstituted Tim23-1 in the absence and presence of 100 nM CoxIV (*cis* and *trans*) at the indicated membrane potentials. Measurements were performed with 250 mM KCl, 0.1 mM CaCl_2 and 10 mM MOPS-Tris, pH 7.0 on either side of the bilayer as outlined for Fig. 1b.

tion (G186D), form a channel across the inner membrane that has a lower sensitivity to presequences¹¹. We generated a recombinant Tim23, Tim23-1, with the same amino acid substitution. Upon reconstitution into liposomes, Tim23-1 revealed a channel activity with a conductance similar to that of wild type Tim23 but with a lower reversal potential ($E_{\text{rev}} = 38 \pm 2.5$ mV; $P_{\text{K}^+} : P_{\text{Cl}^-} = 7:1$) (Fig. 3a). Tim23-1 showed considerably lower reactivity to the CoxIV peptide. At a concentration of 100 nM, the peptide did not affect the Tim23-1 channel activity even at a high membrane potential (Fig. 3b), unlike the results with wild type Tim23 (Fig. 2a,e). Tim23-1 was influenced by the CoxIV peptide only at high (micromolar) concentrations (not shown). The recombinant Tim23-1 therefore shows characteristics also seen with the *tim23-1* mutant mitochondria¹¹.

Characteristics of the presequence translocase

The presequence translocase consists not only of Tim23 but also Tim17, Tim44 and additional components of 14 kDa (Tim14), 33 kDa and 55 kDa (refs 7,9,10,12). The integral membrane proteins Tim17 and Tim23, which are homologous to one another, are both essential for cell viability^{13,14,17–19}. They are present in equimolar amounts and stably associated in the 90 kDa core complex of the translocase^{12,20}, compatible with the hypothesis that these two proteins together form the import channel. However, this model does not fit the observation that yeast mitochondria containing overexpressed Tim23 import significantly more matrix-targeted preprotein than do control mitochondria²¹. Different functions have been reported for Tim23, including roles as a voltage-sensitive presequence receptor^{11,21,22} and as a regulator, but not as a structural element of the multiple conductance channel of the inner membrane¹¹. The observation that purified Tim23 alone forms a presequence-sensitive channel suggested that it would be revealing to compare the channel characteristics of purified Tim23 with that of the multiple conductance channel of the inner membrane of yeast mitochondria.

We sonicated mitochondria, separated inner and outer membrane vesicles and collected highly pure inner membrane vesicles (Fig. 4a, lanes 5 and 12). We fused the inner membrane vesicles with liposomes and then with a planar bilayer. We detected several channel activities, the most frequent being a high-conductance anion channel with two conductance states of 200 pS and 600 pS that specifically responded to inhibitors of the ADP-ATP

carrier, the most abundant protein of the mitochondrial inner membrane (not shown). A channel activity resembling the multiple conductance channel^{8,11} displayed a high cation selectivity and conductance much like the reconstituted Tim23 channel and was the only inner membrane activity sensitive to a mitochondrial presequence (Fig. 4b,c). Antibodies directed against Tim23 inhibited this channel activity of inner membrane vesicles¹¹ (Fig. 4d) as well as the activity of reconstituted Tim23 (Fig. 4f). Preimmune antibodies did not affect the channel activity (Fig. 4e). Moreover, the anti-Tim23 antibodies used here, which were generated against the N-terminal (intermembrane space) domain of Tim23, exerted a strong inhibitory effect on the Tim23 activity only from one side of the membrane (Fig. 4e, legend). This is the same side from which the CoxIV peptide exerted its high-affinity effect (Fig. 2a), supporting the conclusion that reconstituted Tim23 has an asymmetric orientation. The characteristic multiple conductance state, with sub-conductances and a main conductance frequently present in multiples of three, was seen both for the inner membrane activity^{8,11,23} and for reconstituted Tim23 (Fig. 1b) in a comparable pattern. Taken together with the properties of Tim23-1, these findings provide strong evidence that the characteristics of reconstituted Tim23 are comparable to that of the multiple conductance channel, indicating that Tim23 not only regulates¹¹ but also directly forms the multiple conductance channel.

To assess whether Tim23 could form a channel in the mitochondrial inner membrane in the absence of a stable association with Tim17, we used a mutant form, Tim23-2, with a single amino acid substitution in the membrane domain (G112E) that destabilizes the 90 kDa TIM23 complex²⁰. Upon lysis of *tim23-2* mitochondria with digitonin and separation by blue native polyacrylamide electrophoresis (BN-PAGE), Tim23 and Tim17 were lost from the 90 kDa complex (Fig. 5a, lanes 2 and 4). Both proteins probably migrated in the low molecular weight range and thus were not resolved. We determined the total mitochondrial content of Tim23 and Tim17 and their extractability with digitonin and did not find any difference between mutant and wild type (Fig. 5a, lanes 5–10). This indicates that both Tim23 and Tim17 are present in wild type amounts in *tim23-2* mitochondria, but their interaction is destabilized. To quantitatively test the function of the inner membrane protein import channel of *tim23-2* mitochondria, we used saturating amounts of the pre-

articles

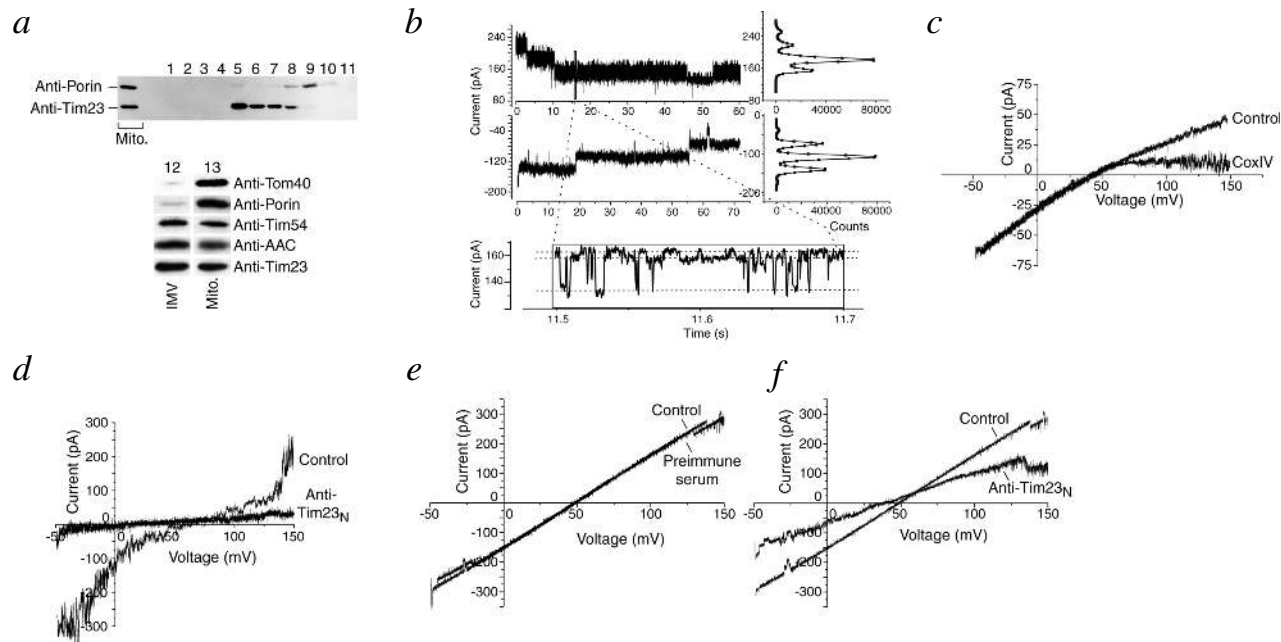


Fig. 4 Tim23-specific characteristics of the inner membrane translocase channel. **a**, Separation of mitochondrial inner and outer membrane vesicles. Upper panel: fractions collected from sucrose gradients were analyzed by immunodecoration with anti-Tim23 and anti-porin antibodies following SDS-PAGE and western blotting. Lower panel: purified inner membrane vesicles (IMV; 5 μ g protein) were analyzed by immunodecoration with mitochondrial proteins (10 μ g protein) as reference. AAC, ADP/ATP carrier. **b**, Current recordings from purified wild type IMV fused with preformed liposomes. The corresponding amplitude histograms are shown on the right. Current recordings were performed in standard symmetrical buffer of 250 mM KCl, 0.1 mM CaCl_2 and 10 mM MOPS-Tris, pH 7.0 at $V_h = +125$ mV (upper) and $V_h = -125$ mV (middle). The lower trace shows a timescale-expanded view of the upper trace. **c**, Current-voltage relationship of a bilayer fused with wild type IMV in the absence or presence (1 μ M) of CoxIV peptide obtained by sweeping the membrane potential (1 mV s^{-1}) from 0 mV to +150 mV and from 0 mV to -50 mV. The buffer was 10 mM MOPS-Tris, pH 7.0, 0.1 mM CaCl_2 with a salt gradient of 250 mM (*cis*)/20 mM KCl (*trans*) across the membrane. **d**, Current-voltage relationship of a bilayer containing purified wild type IMV in the absence (control) or presence of anti-Tim23_N antibodies. In the presence of preimmune antibodies, the current-voltage relationship was superimposable with the control trace. Measurement and asymmetric ionic buffer conditions were as described in (c). Current-voltage relationship of a bilayer containing purified recombinant Tim23 in the **e**, absence of antibody (control) or **f**, in the presence of preimmune or anti-Tim23_N (*trans*). The current-voltage relationship of recombinant Tim23 in the presence of anti-Tim23_N antibody added to the *cis* side of the membrane was largely superimposable with the control trace. Measurement and asymmetric ionic buffer conditions used were as described (Fig. 2a).

protein $b_2\Delta$ -DHFR²⁰. The *tim23-2* mitochondria specifically processed and imported the protein in a membrane potential-dependent manner (Fig. 5a, lanes 16–20) with an efficiency of 50–70% relative to wild type mitochondria. Similar import efficiencies were seen with purified inner membrane vesicles (not shown). The *tim23-2* inner membrane vesicles contained a channel with the same basic characteristics as wild type mitochondria (Fig. 5b,c), with one exception. In the presence of the CoxIV peptide, the E_{rev} of the inner membrane vesicles of *tim23-2* mitochondria was lower, indicating that the channel was less cation selective (Fig. 5c). In contrast, the peptide did not affect the E_{rev} of wild type inner membrane vesicles (Fig. 4c). This provided us with another assay to determine if Tim23 formed the presequence-sensitive channel seen in the mitochondrial inner membrane. We expressed, purified and reconstituted the mutant protein Tim23-2 (Fig. 5d). It showed the same channel characteristics (Fig. 5e,f) as reconstituted wild type Tim23, except that in the presence of the CoxIV peptide, E_{rev} was changed in the same manner as we had seen for total inner membranes of *tim23-2* mitochondria (compare Fig. 5f to 5c). We conclude that Tim23 is responsible for forming the presequence-sensitive channel of the inner membrane. This conclusion, combined with the fact that the TIM channels are four-fold less abundant than the TOM channels and, thus, limiting for the import of presequence-containing preproteins²⁰, explains the observation that overexpression of only Tim23 strongly stimulates the import of these preproteins into mitochondria²¹.

Channel formation by the C-terminal domain of Tim23

Tim23 consists of two domains, a C-terminal hydrophobic domain located in the inner membrane and an N-terminal domain that is exposed to the intermembrane space and binds mitochondrial presequences^{13,17,21,22,24} (Fig. 6a). Surprisingly, it has been reported that Tim23 is integrated into the outer membrane through its N-terminal domain²⁵. Therefore, we investigated which domain of Tim23 forms the cation-selective channel identified here. We expressed and purified both Tim23 domains separately (Fig. 6a). Although Tim23_N did not form detectable channels, reconstituted Tim23_C formed a channel with the same basic characteristics as were seen for full-length Tim23 (Fig. 6b). The cation selectivity of Tim23_C was lower ($E_{\text{rev}} = 27$ mV; $P_{\text{K}^+} : P_{\text{Cl}^-} = 3.8:1$), however, and its affinity to a presequence peptide was markedly lower than that of full-length Tim23. The CoxIV peptide still caused channel flickering and current block, but only at micromolar concentrations (Fig. 6c); no effect was detected at nanomolar concentrations. We conclude that Tim23_N is required for the selectivity and high-affinity influence of a presequence on the channel activity of Tim23_C.

Estimated pore diameter

The diameter of the Tom40 translocation pore has been experimentally estimated at ~ 20 – 22 Å, indicating that a polypeptide in an α -helical conformation can easily be translocated through it and that two α -helices (for example, a preprotein in a loop formation) could even be translocated together^{5,6,26}. The rela-

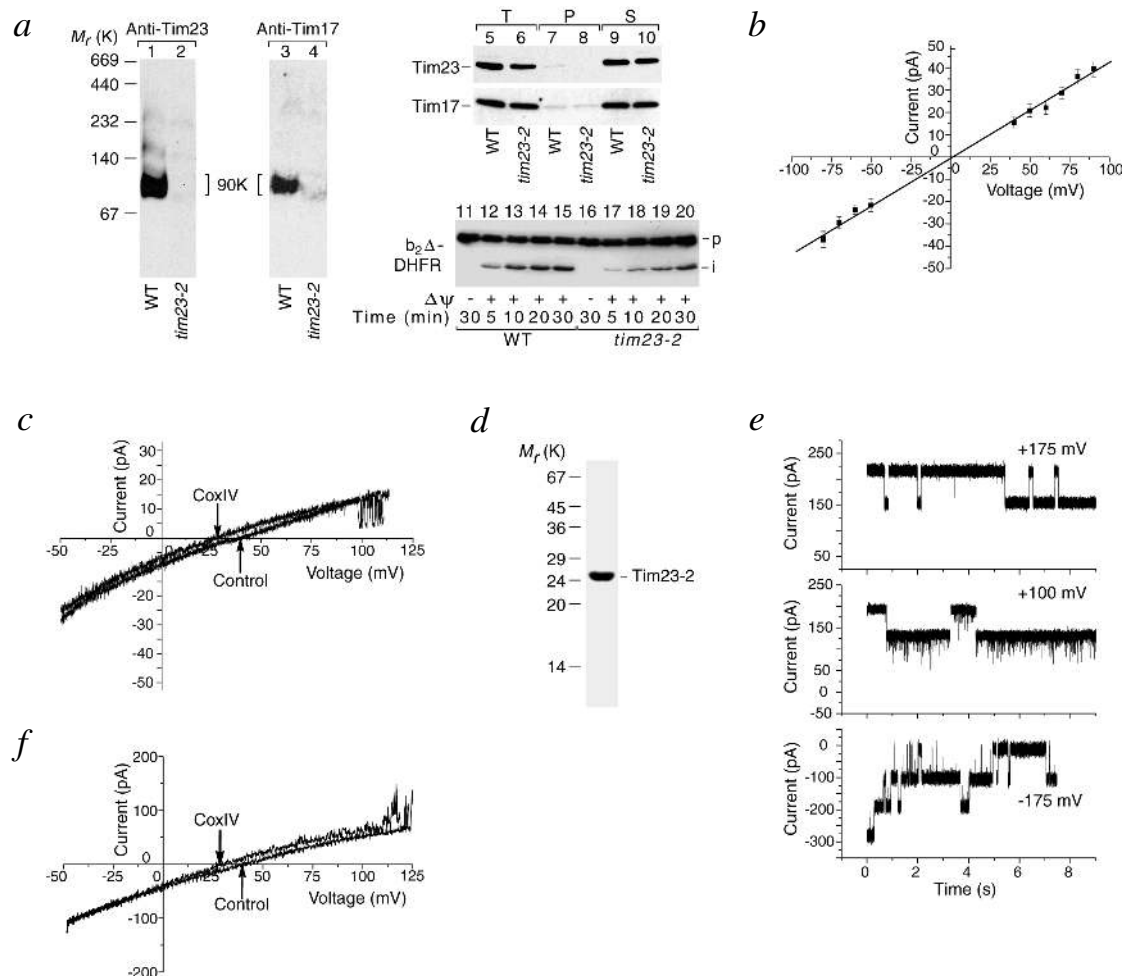


Fig. 5 The translocase channel is present in *tim23-2* mutant mitochondria despite a destabilization of the Tim23–Tim17 interaction. **a**, The 90 kDa core complex is strongly destabilized in *tim23-2* mitochondria. Mitochondria were isolated from wild type (WT) and *tim23-2* yeast and analyzed by immunodecoration with anti-Tim23 and anti-Tim17 antibodies following separation on BN-PAGE (lanes 1–4; after lysis of the mitochondria with 1% digitonin) or on SDS-PAGE (lanes 5–10): lanes 5,6, total (T) mitochondrial protein; lanes 7,8: insoluble protein pellet (P) following solubilization of mitochondria with 1% digitonin; lanes 9,10: digitonin-solubilized (S) mitochondrial protein (precipitated with TCA). Lanes 11–20: mitochondria with destabilized 90 kDa core complex import saturating amounts of preprotein. Purified $b_2\Delta$ -DHFR (640 pmol mg^{-1} mitochondrial protein) was imported into isolated wild type or *tim23-2* mitochondria in the presence or absence of a membrane potential ($\Delta\psi$). Precursor (p) and intermediate (i) preprotein was detected by immunodecoration with anti-DHFR antibodies after separation of reisolated mitochondria by SDS-PAGE and subsequent western blotting. **b**, Current–voltage relationship deduced from the single-channel conductance from bilayers fused with *tim23-2* IMV with 250 mM KCl, 0.1 mM $CaCl_2$, 10 mM MOPS-Tris, pH 7.0 on either side of the bilayer (average of at least three independent bilayers). **c**, Current–voltage recording from a bilayer fused with *tim23-2* IMV in the absence or presence of 1 μ M CoxIV peptide obtained by sweeping the membrane potential (1 $mV s^{-1}$) from 0 mV to +110 mV and from 0 mV to –50 mV. The *cis* compartment contained 250 mM KCl, 0.1 mM $CaCl_2$, 10 mM MOPS-Tris, pH 7.0 and the *trans* compartment 20 mM KCl, 0.1 mM $CaCl_2$, 10 mM MOPS-Tris, pH 7.0. **d**, Purity of recombinant Tim23-2 assessed by SDS-PAGE with Coomassie brilliant blue staining. **e**, Single-channel current traces of purified Tim23-2 at different membrane voltages as indicated. **f**, Current–voltage recording from a bilayer containing purified Tim23-2 in the absence or presence of 1 μ M CoxIV peptide obtained by sweeping the membrane potential (1 $mV s^{-1}$) from 0 mV to +125 mV and from 0 mV to –50 mV (conditions as for **c**).

tively large size of the outer membrane translocation channel was puzzling in light of functional studies indicating that pre-proteins are substantially unfolded during translocation, so that they should cross the membranes in the form of linear chains²⁷. Only indirect information is available about the pore size of the TIM23 translocase. Gold particles of 20 Å diameter can be transported across the outer membrane but are strongly inhibited in translocation across the inner membrane²⁶. Assuming a cylindrical protein channel with a five-fold higher resistance than the bulk medium²⁸ and using the conductance of the reconstituted Tim23 channel (and the corresponding inner membrane channel), the calculated mean pore diameter is ~18–19 Å. To obtain more direct evidence of the effective pore diameter, we used the polymer-exclusion method^{28,29} with poly-

ethylene glycol of different sizes. The conductance ratio dependence on the polymer size leads to a calculated external (vestibule) diameter of ~24 Å and an inner (restriction zone) diameter of ~13 Å (Fig. 7). Thus, the Tim23 channel is not simply a cylindrical pore; rather, its internal and external diameters differ considerably. At its narrowest point, the Tim23 channel is smaller than both the Tom40 channel^{5,6,26} and the functional translocon of the endoplasmic reticulum (~20–50 Å)^{30–32} but is similar to the average diameter of the polypeptide exit channel of the ribosome large subunit (15 Å)³³. The restriction zone diameter of the Tim23 channel is just large enough to accommodate one polypeptide chain in an α -helical conformation but not large enough to contain two α -helices at the same time. This suggests that the mechanism of protein translocation

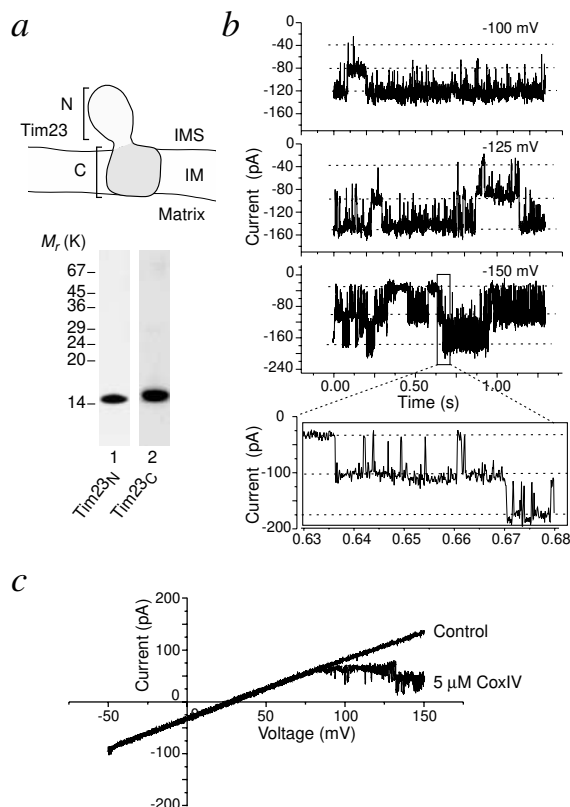
articles

Fig. 6 The C-terminal domain of Tim23 forms the channel. **a**, Structural and functional domains of Tim23. Purity, as determined by SDS-PAGE with Coomassie brilliant blue staining, of recombinant Tim23 N-terminal domain (Tim23_N) and Tim23 C-terminal domain (Tim23_C). **b**, Current recordings from a bilayer containing active Tim23_C channels at different membrane potentials as indicated. Both bath chambers contained 250 mM KCl, 0.1 mM CaCl₂ and 10 mM MOPS-Tris, pH 7.0. The lower trace indicates a timescale-magnified view from the trace above ($V_m = -150$ mV). **c**, Current recording from a bilayer containing active Tim23_C channels over a range of applied voltages (increment 1 mV s⁻¹). The *cis* compartment contained 250 mM KCl, 0.1 mM CaCl₂ and 10 mM MOPS-Tris, pH 7.0 and the *trans* compartment 20 mM KCl, 0.1 mM CaCl₂ and 10 mM MOPS-Tris, pH 7.0. Recordings in the absence (control) and presence of 5 μ M CoxIV in the *trans* compartment. At CoxIV peptide concentrations <1 μ M, the current-voltage relationships were superimposable with the control trace.

across the inner membrane requires polypeptides to unfold at least to the level of individual α -helices.

Conclusions

We report that Tim23 forms a channel in the presence of the presequence translocase of the mitochondrial inner membrane. The successful reconstitution of purified Tim23 into a lipid bilayer described here has allowed a direct measure of its properties and, together with the use of mutants, an assessment of its role in mitochondria. The reconstituted channel exhibits all the characteristics of the physiological channel, including high cation selectivity, large multiple conductance^{8,11} and an effective pore size that requires unfolding of the polypeptide chain during translocation. Bauer *et al.*²¹ reported that a membrane potential promotes dimerization of the N-terminal domains of Tim23 and an interaction with presequences. Our reconstitution of the Tim23 channel shows that the channel can be activated either by a rapid increase of the membrane potential alone or by the combined presence of both a presequence and a membrane potential of sufficient magnitude. The latter combination is probably the typical physiological situation in mitochondria. The membrane potential thus promotes protein import by several means, including an electrophoretic effect on the positively charged presequences¹⁻⁴ and direct stimulation of both the receptor function and channel activity of Tim23. Upon prolonged exposure to a membrane potential in the absence of preproteins, the Tim23 channel tends to close; this probably helps to maintain an electrochemical gradient across the inner membrane. The membrane channel is formed by the C-terminal domain of Tim23. Tim17 is weakly homologous to this domain^{13,14,17-19}, indicating



that Tim17 might also form a channel, although functional expression and reconstitution of this protein alone has not been possible so far. It is evident, however, that Tim23 represents the presequence-sensitive channel of the mitochondrial inner membrane. Only Tim23 contains a large N-terminal domain exposed to the intermembrane space that binds presequences with high affinity^{13,17,19,21,22}; Tim17 lacks such a domain. Both functions of Tim23, as presequence receptor and channel, are intimately linked, because the high-affinity influence of a presequence on the channel formed by the C-terminal domain is mediated by the N-terminal domain. Tim23 thus offers an efficient means by which presequence recognition at the inner mitochondrial membrane can be coupled to transport of the preprotein across the membrane.

Methods

Expression and reconstitution of Tim23. Yeast Tim23 and the mutant forms Tim23-1 and Tim23-2 were expressed from the plasmid pET10N with an N-terminal His₁₀-tag in the *E. coli* strain C43 (DE3)³⁴. After induction with 1 mM isopropyl- β -D-thiogalactopyranoside (IPTG) (3 h), cells were lysed and inclusion bodies were isolated⁵ and denatured in 8 M urea, 100 mM NaH₂PO₄, 10 mM Tris-HCl,

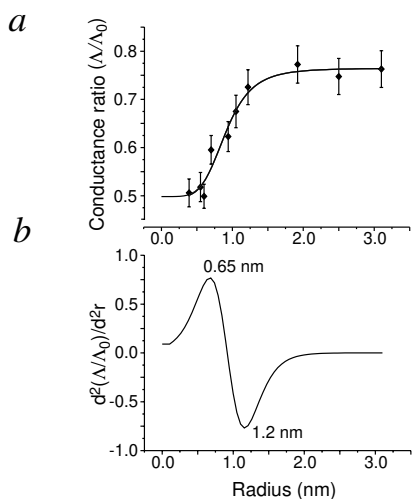


Fig. 7 Estimation of the Tim23 pore size by the polymer exclusion method. **a**, Ratio of the Tim23 channel conductance without (Δ_0) and after (Δ) partition into the pore of polyethylene glycol (PEG) of different hydrodynamic radii (ranging from PEG 200 to PEG 6000) and additional smaller nonelectrolytes²⁹. The buffer contained 15% (w/v) nonelectrolyte, 100 mM KCl and 10 mM MOPS-Tris, pH 7.0, on either side of the bilayer. Data points are averages of at least three independent bilayers. The line shows the fit of the data according to reported methods³⁵. **b**, Second derivative of the data fit from the upper panel, showing the first turning point where partitioning into the inner pore of the small nonelectrolytes of increasing radius becomes restricted. The second turning point indicates the size of the large nonelectrolytes of decreasing radius that are still able to enter the outer parts of the channel.



pH 8.0. The mixture was applied to NiNTA-agarose and the adsorbent washed sequentially with 8 M urea, 100 mM NaH_2PO_4 and 10 mM Tris-HCl, pH 6.3 and 80 mM imidazole and with 8 M urea, 100 mM NaH_2PO_4 , 10 mM Tris-HCl, pH 5.9, then eluted with 8 M urea, 100 mM NaH_2PO_4 and 10 mM Tris-HCl, pH 4.5. Tim23_N (amino acid residues 1–96) was expressed from pET10C with a C-terminal His₆-tag in C43 (DE3). Tim23_C (residues 92–222) was expressed from pET10N in *E. coli* strain BL21-Codon Plus (DE3)-RIL (Stratagene). *E. coli* cells were lysed with 6 M guanidinium chloride, 100 mM Na_2HPO_4 , 10 mM Tris-HCl, pH 8.0, and Tim23_N and Tim23_C were purified via NiNTA-agarose chromatography. Wash and elution buffers were as for full-length Tim23. To raise antibodies against the N-terminal domain of Tim23, the purified recombinant domain Tim23_N was used to immunize rabbits.

Reconstitution into liposomes was achieved by the dialysis technique. Preformed small, unilamellar liposomes obtained from purified azolectin (Sigma, type IV S)⁵ were lysed in Mega-9 buffer (80 mM Mega-9, 10 mM MOPS-Tris, pH 7.0, and 1 mM EDTA), and Tim23 (~1 mg ml⁻¹) in urea was diluted ~10-fold into the mixture to yield a lipid-to-protein ratio of 10:1 (w/w). Proteoliposomes were formed following dialysis against 10 mM KCl, 1 mM CaCl_2 and 10 mM MOPS-Tris, pH 7.0.

Inner membrane vesicles. Isolated yeast mitochondria were adjusted to a protein concentration of 10 mg ml⁻¹. Mitochondria were swollen for 30 min on ice by 10-fold dilution with 20 mM HEPES-KOH, pH 7.2 and 1 mM PMSF. After restoration of isotonic conditions and sonication, crude vesicles were isolated by centrifugation at 20,000 g. Pellets were resuspended in 5 mM HEPES-KOH, pH 7.2, 10 mM KCl and 1 mM PMSF and loaded onto discontinuous 0.85–1.6% (w/v) sucrose gradients. Following centrifugation for 16 h at 100,000g, vesicles were harvested and subjected to SDS-PAGE analysis. The vesicles were mixed 1:1 (v/v) with preformed small, unilamellar liposomes and fused by sonication five times for 30 s each in a 20 ml water bath mounted in a microtip-equipped Branson sonifier. The fused vesicles were exposed to one freeze/thaw cycle and sonicated again for 30 s before being subjected to electrophysiological measurements.

Electrophysiological measurements. The painting technique was used to form planar lipid bilayers^{5,16}. The *cis* chamber solution was changed to asymmetrical concentrations (*cis* chamber: 250 mM KCl, 1 mM CaCl_2 and 10 mM MOPS-Tris, pH 7.0) once a stable bilayer was formed in symmetrical solutions of 20 mM KCl and 10 mM MOPS-Tris, pH 7.0. The liposomes were added to the *cis* compart-

ment directly below the bilayer. The standard buffer for symmetrical measurements was 250 mM KCl, 0.1 mM CaCl_2 and 10 mM MOPS-Tris, pH 7.0. Agar bridges containing 2 M KCl were used to connect the Ag/AgCl electrodes to the chambers. The electrode of the *trans* compartment (reference chamber for reported membrane potentials) was directly connected to the headstage (Cv-5-1GU) of a current amplifier (Geneclamp 500, Axon Instruments). Amplified currents were recorded using a Digidata 1200 A/D converter. For analysis, a self-developed Microsoft Windows-based analysis software (SCIP, single-channel investigation program) was used in combination with Origin 6.0 (Microcal Software).

BN-PAGE and protein import into mitochondria. For BN-PAGE, mitochondria (50 µg) were resuspended in 50 µl of ice-cold digitonin buffer (1% (w/v) digitonin, 20 mM Tris-HCl, pH 7.4, 0.1 mM EDTA, 50 mM NaCl, 10% (v/v) glycerol and 1 mM PMSF), incubated on ice for 15 min and then centrifuged at 12,000g, 4 °C for 15 min. Sample buffer (5 µl) was added (5% (w/v) Coomassie brilliant blue G-250, 100 mM Bis-Tris, pH 7.0 and 500 mM 6-aminocaproic acid) and the samples were then separated on 6–16.5% polyacrylamide gradient gels at 4 °C (ref. 20).

The preprotein b₂Δ-DHFR was purified as described²⁰. Isolated yeast mitochondria were resuspended in import buffer (3% (w/v) BSA, 250 mM sucrose, 5 mM MgCl_2 , 80 mM KCl, 5 mM methionine, 10 mM MOPS-KOH, pH 7.2) and supplemented with 2 mM each of ATP, NADH and GTP. Just before import, the preprotein was diluted to 0.16 µM in import buffer (minus BSA) and the sample clarified by centrifugation. Following import at 25 °C, mitochondria were reisolated, washed in 250 mM sucrose, 1 mM EDTA and 10 mM MOPS-KOH, pH 7.2, and then separated by 14% SDS-PAGE. Import was assessed by immunodecoration with an anti-DHFR following transfer to polyvinylidene difluoride (PVDF) membrane²⁰.

Acknowledgments

We are grateful to J. Walker for the *E. coli* strain C43 (DE3), R. Jensen for antibody against Tim17, B. Guiard, J. H. Lim, A. Chacinska and W. Voos for b₂Δ-DHFR, K. Model and C. Meisinger for technical advice, and H. Müller for expert technical assistance. This work was supported by the Deutsche Forschungsgemeinschaft, the Sonderforschungsbereich 388, the Fonds der Chemischen Industrie/BMBF (N.P.), the Sonderforschungsbereich 431 (R.W.) and a long-term fellowship from the Alexander von Humboldt Foundation (K.N.T.).

Received 19 June, 2001; accepted 4 October, 2001.



articles

1. Schatz, G. & Dobberstein, B. Common principles of protein translocation across membranes. *Science* **271**, 1519–1526 (1996).
2. Jensen, R.E. & Johnson, A.E. Protein translocation: is Hsp70 pulling my chain? *Curr. Biol.* **9**, R779–R782 (1999).
3. Bauer, M.F., Hofmann, S., Neupert, W. & Brunner, M. Protein translocation into mitochondria: the role of TIM complexes. *Trends Cell Biol.* **10**, 25–31 (2000).
4. Matouschek, A., Pfanner, N. & Voos, W. Protein unfolding by mitochondria: the Hsp70 import motor. *EMBO Rep.* **1**, 404–410 (2000).
5. Hill, K. *et al.* Tom40 forms the hydrophilic channel of the mitochondrial import pore for preproteins. *Nature* **395**, 516–521 (1998).
6. Künkele, K.-P. *et al.* The preprotein translocation channel of the outer membrane of mitochondria. *Cell* **93**, 1009–1019 (1998).
7. Ryan, K.R. & Jensen, R.E. Mas6p can be cross-linked to an arrested precursor and interact with other proteins during mitochondrial protein import. *J. Biol. Chem.* **268**, 23743–23746 (1993).
8. Lohret, T.A. & Kinnally, K.W. Targeting peptides transiently block a mitochondrial channel. *J. Biol. Chem.* **270**, 15950–15953 (1995).
9. Berthold, J. *et al.* The MIM complex mediates preprotein translocation across the mitochondrial inner membrane and couples it to the mt-Hsp70/ATP driving system. *Cell* **81**, 1085–1093 (1995).
10. Blom, J., Dekker, P.J.T. & Meijer, M. Functional and physical interactions of components of the yeast mitochondrial inner-membrane import machinery (MIM). *Eur. J. Biochem.* **232**, 309–314 (1995).
11. Lohret, T.A., Jensen, R.E. & Kinnally, K.W. Tim23, a protein import component of the mitochondrial inner membrane, is required for normal activity of the multiple conductance channel, MCC. *J. Cell Biol.* **137**, 377–386 (1997).
12. Moro, F., Srrenberg, C., Schneider, H.-C., Neupert, W. & Brunner, M. The TIM17-23 preprotein translocase of mitochondria: composition and function in protein transport into the matrix. *EMBO J* **18**, 3667–3675 (1999).
13. Emtage, J.L.T. & Jensen, R.E. MAS6 encodes an essential inner membrane component of the yeast mitochondrial protein import pathway. *J. Cell Biol.* **122**, 1003–1012 (1993).
14. Dekker, P.J.T. *et al.* Identification of MIM23, a putative component of the protein import machinery of the mitochondrial inner membrane. *FEBS Lett.* **330**, 66–70 (1993).
15. Allison, D.S. & Schatz, G. Artificial mitochondrial presequences. *Proc. Natl Acad. Sci. USA* **83**, 9011–9015 (1986).
16. Böltter, B., Söll, J., Hill, K., Hemmler, R. & Wagner, R. A rectifying ATP-regulated solute channel in the chloroplastic outer envelope from pea. *EMBO J* **18**, 5505–5516 (1999).
17. Kübrich, M. *et al.* The polytopic mitochondrial inner membrane proteins MIM17 and MIM23 operate at the same preprotein import site. *FEBS Lett.* **349**, 222–228 (1994).
18. Maarse, A.C., Blom, J., Keil, P., Pfanner, N. & Meijer, M. Identification of the essential yeast protein MIM17, an integral mitochondrial inner membrane protein involved in protein import. *FEBS Lett.* **349**, 215–221 (1994).
19. Ryan, K.R., Menold, M.M., Garrett, S. & Jensen, R.E. SMS1, a high-copy suppressor of the yeast *mas6* mutant, encodes an essential inner membrane protein required for mitochondrial protein import. *Mol. Biol. Cell* **5**, 529–538 (1994).
20. Dekker, P.J.T. *et al.* The Tim core complex defines the number of mitochondrial translocation contact sites and can hold arrested preproteins in the absence of matrix Hsp70-Tim44. *EMBO J* **16**, 5408–5419 (1997).
21. Bauer, M.F., Srrenberg, C., Neupert, W. & Brunner, M. Role of Tim23 as voltage sensor and presequence receptor in protein import into mitochondria. *Cell* **87**, 33–41 (1996).
22. Komiya, T. *et al.* Interaction of mitochondrial targeting signals with acidic receptor domains along the protein import pathway: evidence for the 'acid chain' hypothesis. *EMBO J* **17**, 3886–3898 (1998).
23. Zoratti, M. & Szabo, I. Electrophysiology of the inner mitochondrial membrane. *J. Bioenerg. Biomembr.* **26**, 543–553 (1994).
24. Ryan, K.R., Leung, R.S. & Jensen, R.E. Characterization of the mitochondrial inner membrane translocase complex: the Tim23p hydrophobic domain interacts with Tim17p but not with other Tim23p molecules. *Mol. Cell. Biol.* **18**, 178–187 (1998).
25. Donzeau, M. *et al.* Tim23 links the inner and outer mitochondrial membranes. *Cell* **101**, 401–412 (2000).
26. Schwartz, M.P. & Matouschek, A. The dimensions of the protein import channels in the outer and inner mitochondrial membranes. *Proc. Natl Acad. Sci. USA* **96**, 13086–13090 (1999).
27. Passow, J., Hartl, F.-U., Guiard, B., Pfanner, N. & Neupert, W. Polypeptides traverse the mitochondrial envelope in an extended state. *FEBS Lett.* **275**, 190–194 (1990).
28. Smart, O.S., Breed, J., Smith, G.R. & Sansom, M.S. A novel method for structure-based prediction of ion channel conductance properties. *Biophys. J.* **72**, 1109–1126 (1997).
29. Krasnikow, O.V., Sabirov, R.Z., Ternovsky, V.L., Merzliak, P.G. & Muratkhodjaev, J.N. A simple method for the determination of the pore radius of ion channels in planar lipid bilayer membranes. *FEMS Microbiol. Immunol.* **5**, 93–100 (1992).
30. Hamman, B.D., Hendershot, L.M. & Johnson, A.E. BiP maintains the permeability barrier of the ER membrane by sealing the luminal end of the translocon pore before and early in translocation. *Cell* **92**, 747–758 (1998).
31. Beckmann, R. *et al.* Alignment of conduits for the nascent polypeptide chain in the ribosome–Sec61 complex. *Science* **278**, 2123–2126 (1997).
32. Ménétret, J.-F. *et al.* The structure of ribosome-channel complexes engaged in protein translocation. *Mol. Cell* **6**, 1219–1232 (2000).
33. Nissen, P., Hansen, J., Ban, N., Moore, P.B. & Steitz, T.A. The structural basis of ribosome activity in peptide bond synthesis. *Science* **289**, 920–930 (2000).
34. Miroux, B. & Walker, J.E. Over-production of proteins in *Escherichia coli*: mutant hosts that allow synthesis of some membrane proteins and globular proteins at high levels. *J. Mol. Biol.* **260**, 289–298 (1996).
35. Bezrukov, S.M. & Kasianowicz, J.J. The charge state of an ion channel controls neutral polymer entry into its pore. *Eur. Biophys. J.* **26**, 471–476 (1997).